atmosphere

MDPI

Article

Investigating the Atmospheric Sources and Sinks of Perfluorooctanoic Acid Using a Global Chemistry Transport Model

Rayne Holland [1], M. Anwar H. Khan [1], Rabi Chhantyal-Pun [1], Andrew J. Orr-Ewing [1], Carl J. Percival [2], Craig A. Taatjes [3] and Dudley E. Shallcross [1,4,*]

1 School of Chemistry, University of Bristol, Bristol BS8 1TS, UK; rh15078@bristol.ac.uk (R.H.); anwar.khan@bristol.ac.uk (M.A.H.K.); rc13564@bristol.ac.uk (R.C.-P.); a.orr-ewing@bristol.ac.uk (A.J.O.-E.)
2 NASA Jet Propulsion Laboratory, California Institute of Technology, 4800 Oak Grove Dr, Pasadena, CA 91109, USA; carl.j.percival@jpl.nasa.gov
3 Combustion Research Facility, Mailstop 9055, Sandia National Laboratories, Livermore, CA 94551, USA; cataatj@sandia.gov
4 Department of Chemistry, University of the Western Cape, Robert Sobukwe Road, 7535 Bellville, South Africa
* Correspondence: d.e.shallcross@bris.ac.uk; Tel.: +44-117-928-7796

Received: 22 March 2020; Accepted: 17 April 2020; Published: 19 April 2020

Abstract: Perfluorooctanoic acid, PFOA, is one of the many concerning pollutants in our atmosphere; it is highly resistant to environmental degradation processes, which enables it to accumulate biologically. With direct routes of this chemical to the environment decreasing, as a consequence of the industrial phase out of PFOA, it has become more important to accurately model the effects of indirect production routes, such as environmental degradation of precursors; e.g., fluorotelomer alcohols (FTOHs). The study reported here investigates the chemistry, physical loss and transport of PFOA and its precursors, FTOHs, throughout the troposphere using a 3D global chemical transport model, STOCHEM-CRI. Moreover, this investigation includes an important loss process of PFOA in the atmosphere via the addition of the stabilised Criegee intermediates, hereby referred to as the "Criegee Field." Whilst reaction with Criegee intermediates is a significant atmospheric loss process of PFOA, it does not result in its permanent removal from the atmosphere. The atmospheric fate of the resultant hydroperoxide product from the reaction of PFOA and Criegee intermediates resulted in a ≈0.04 Gg year^{-1} increase in the production flux of PFOA. Furthermore, the physical loss of the hydroperoxide product from the atmosphere (i.e., deposition), whilst decreasing the atmospheric concentration, is also likely to result in the reformation of PFOA in environmental aqueous phases, such as clouds, precipitation, oceans and lakes. As such, removal facilitated by the "Criegee Field" is likely to simply result in the acceleration of PFOA transfer to the surface (with an expected decrease in PFOA atmospheric lifetime of ≈10 h, on average from ca. 80 h without Criegee loss to 70 h with Criegee loss).

Keywords: Criegee intermediates; perfluorooctanoic acid; global budget; atmospheric lifetime

1. Introduction

Perfluorinated carboxylic acids (PFCAs) constitute a class of organic acids with a general formula of $C_nF_{(2n+1)}COOH$, which, despite being exclusively anthropogenically generated, are found to be ubiquitous in the environment [1]. Over recent years, these have become compounds of significant scientific and regulatory interest due to their bio-accumulative nature [2,3] and suspected toxicity [4,5].

Of the PFCAs, the C_8 compound—termed perfluorooctanoic acid (PFOA)—is predicted to have had the highest total emissions, exceeding the second most emitted PFCA by an order of magnitude [6],

due to its extensive use in the fluoropolymer industry [7]. As a result of its high emissions and its bio-accumulative nature, PFOA is the most widely encountered PFCA and is found in significant concentrations in humans [8] and biota [9,10]. This is particularly concerning in view of the suspected carcinogenicity of the compound [11]. Furthermore, PFOA—and its precursors—have been found to contaminate urban, indoor and remote environments [12,13]. As a result of this, industrial production of PFOA was voluntarily phased out by most relevant companies in 2015 [14] and PFOA and its salts have recently been added to Annexe A of the Stockholm Convention for persistent organic pollutants (POPs) [15].

Despite these efforts to reduce direct emissions of PFOA, an alternative pathway of environmental contamination remains operational via the degradation of fluorotelomer alcohols (FTOHs); specifically, 8:2 FTOH which oxidatively degrades in the atmosphere to yield PFOA [16–18]. FTOHs have been and continue to be used extensively in industry for a range of purposes from stain repellents to firefighting foams [19]. Given the short atmospheric lifetime of PFOA itself (as a result of facile removal by atmospheric deposition processes), it is likely that this route represents the primary contributor to the contamination of remote environments. In contrast to PFOA, which only has an atmospheric lifetime of approximately 12 days [16], FTOH may persist in the atmosphere for upwards of 20 days, allowing significant long-range tropospheric transport [20].

As alluded to previously, wet and dry deposition processes are believed to dominate the atmospheric fate of PFOA, given its slow oxidation and inefficient photolysis processes [21,22]. However, a recent report suggests that reaction with Criegee intermediates (CIs) is also likely to be significant in determining the atmospheric fate of PFOA, though it is important to note that this study did not explicitly investigate the impact of this loss process on a global scale [23]. Previous investigations surrounding PFOA and its related compounds include, but are not limited to: modelling pathways of PFOA to the Arctic [12]; biological monitoring of PFOA [24]; a global survey of PFOA in oceans [2]; global fate and transport modelling of PFOA from direct sources [25]; and modelling 8:2 FTOH degradation as a potential source of PFOA [16]. However, as no study has currently been conducted that fully accounts for the atmospheric fate of PFOA, including the implications of CI-mediated oxidation; there remains a clear gap in the literature.

CIs are zwitterionic carbonyl oxide intermediates generated by the ozonolysis of alkenes in the atmosphere. These intermediates are high in energy and either rapidly decompose by unimolecular decomposition or stabilise via collisional energy loss with a "bath" gas (most likely O_2 or N_2) to generate thermally stable forms of the intermediate hereinafter referred to as SCIs. These stabilised intermediates may exist on a significant timescale and in significant concentrations (approximately 10^4–10^5 cm^{-3} in the surface layer) [26–28], as such their atmospheric fates are important to consider.

A number of previous studies elucidated the reactions of SCIs with a selection of trace gases and atmospheric pollutants and found them to be significant [27,29,30]. In fact, the rate coefficients for organic and inorganic acids have been shown to approach or even exceed the gas kinetic limit [31–34]. Taatjes et al. [23] have recently experimentally determined the rate coefficient of PFOA's reaction with the simplest SCI, CH_2OO, to be $(4.9 \pm 0.8) \times 10^{-10}$ cm^3 s^{-1}. Operating under the assumption that reactions of PFOA with all common SCIs occur at similar rates, it is clear that this atmospheric loss process is likely to be significant in determining the overall fate of PFOA in the atmosphere.

It is also important to consider the atmospheric fate of the SCI-mediated products. Taatjes et al. [23] and Chhantyal-Pun et al. [34] have shown that the simplest SCI, CH_2OO, reacts with halogenated carboxylic acids to produce a hydroperoxide ester (HPE). The HPE product likely undergoes reaction with OH in the atmosphere. Following this oxidation, gaseous HPE may undergo further oxidation to either reform PFOA (with formic acid as a side product) or form carbon dioxide and hydrofluoric acid, resulting in the permanent destruction of PFOA [23] (see Figure S1). Whilst exact contributions of each route are not explicitly reported in the literature, it is generally agreed that the former oxidation route is likely to dominate, and as such the majority of HPE in the atmosphere will go on to reform

PFOA [23,35]. With ≈80% of HPE reforming PFOA in the atmosphere, it is expected that atmospheric degradation of the former does not provide a significant long-term sink for the latter.

Previous work is significantly improved here via explicit numerical modelling of the fates of the 17 most common SCIs benchmarked with the most recently available laboratory measurements and quantum chemistry calculations, hereby referred to as the "Criegee Field", into the global tropospheric model STOCHEM-CRI [28]. In doing so, we are able to better quantify the contribution of SCI-mediated loss on the global budget of PFOA.

2. Modelling

STOCHEM is the name of a Lagrangian tropospheric chemical transport 3D model which operates such that atmospheric transport processes and individual chemical reactions are treated independently (which in turn allows chemistry timesteps to be determined locally) [36]. Driven by archived meteorological data from the UK Meteorological Office, STOCHEM is an "offline" model that functions at the atmospheric resolution of the Meteorological Office unified model (1.25° longitude × 0.83° latitude × 12 uneven vertical levels) [37]. The data outputs include: pressure, temperature, humidity, interpolated wind data, tropopause height, cloud amount, precipitation, boundary layer height and surface parameters [38]. The meteorological module of STOCHEM has been discussed in detail previously [36] and updates can be found in Derwent et al. [39].

This investigation utilises the reduced chemical mechanism CRI v2-R5, the advancement of which has been reported by Jenkin et al. [40] and Watson et al. [41] with further amendments reported by Utembe et al. [42,43] and Khan et al. [44]. The development of this mechanism involved species-specific, box model simulations in addition to optimisation using the Master Chemical Mechanism version 3.1 (MCM v3.1) with ozone generation set as the key principle [43,45].

In the first instance, simulations contained 50,000 air parcels where each air parcel accommodated individual concentrations of a total 231 species; which compete in 532 chemical reactions. Chemical processes (formation/loss reactions and photochemical dissociations) occur within the air parcels in addition to individual emissions, depositions, convection and further removal processes of all species. The individual photolysis rates are calculated according to Percival et al. [46]. Modifications made in this investigation include the addition of the direct emissions and complete atmospheric fate of PFOA and 8:2 FTOH along with the addition of the "Criegee Field."

Global emission fluxes for PFOA and its primary precursor, 8:2 FTOH (simply referred to as FTOH), were added according to Armitage et al. [25] (0.005 Tg year^{-1}) and Wallington et al. [16] (0.001 Tg year^{-1}), respectively. The relevant compounds are emitted via anthropogenic routes exclusively [23]. Physical and chemical removal processes of these species were also included to properly represent their atmospheric fate. Dry and wet deposition represent all physical removal processes in the STOCHEM model and a full explanation for how these processes are represented can be found in Von Kuhlmann [47]. Wet and dry deposition of PFOA are particularly important because of its high solubility and large size. The rate of wet deposition depends on the dynamic and convective deposition fluxes and is therefore species-specific. Deposition velocities for PFOA were extracted from Wallington et al. [16]. whilst dynamic and convective scavenging coefficients were calculated using the Henrys Law constant vs. Scavenging coefficient correlation (where Henry's Law constants and scavenging coefficients were extracted from Sander et al. [48] and Penner et al. [49], respectively). The dry deposition velocities of 1.9 mm s^{-1} over land and ocean and the wet deposition parameters, dynamic scavenging of 1.9 cm^{-1} and convective scavenging of 3.8 cm^{-1} were used for PFOA in all simulations. FTOH is assumed not to undergo any significant deposition processes and as such none were included in the updated chemical module [50].

Addition of the Criegee Field involved the inclusion of 17 individual SCIs along with explicit formation and loss processes for each. Emission data for the relevant alkenes (ethene, propene, trans-but-2-ene, isoprene, α-pinene and β-pinene) are already accounted for in the STOCHEM model, and as such, they can be found in the full emission inventory reported by Khan et al. [51]. Inclusion of the

"Criegee Field" required addition of the ozonolysis reactions of each of the precursor alkenes for which the rate coefficients were taken from the Master Chemical Mechanism [52] (see Table S2). The yields for SCI from ozonolysis of various alkenes were taken from previous study of McGillen et al. [53]. The loss processes included for each SCI in this model are unimolecular reactions and the reactions with water and water dimer (More details can be found in Chhantyal-Pun et al. [28] and Table S3). The chemical loss processes (i.e., unimolecular decomposition and reaction with water and water dimer) strongly dominate resulting in the very short atmospheric lifetime of SCIs. Additional minor loss processes of SCIs have not been included to reduce computational costs. As all SCIs included are expected to have similar reaction rates with PFOA, inclusion of individual reactions would be computationally inefficient. As such, all individual SCIs included are grouped into a singular class labelled "SCI." This class accounts for the total concentration of all the included SCIs and assumes a consistent rate of reaction for all SCI's with PFOA (4.9×10^{-10} cm^3 s^{-1}) [23]. Following the inclusion of the "Criegee Field," each air parcel now contains concentrations of a total of 249 species that compete in 582 chemical reactions and utilise a time-step of 5 min.

A range of simulations (STOCH-Base, STOCH-DE, STOCH-CI and STOCH-HPE) were performed during this investigation. A collection of the basic features of the simulations and the differences between individual simulations can be found in Table 1. "STOCH-Base" employed the CRI mechanism with the only modifications appearing in the emission inventory. The only emission modification is the addition of global FTOH emission data; as such, the only source of PFOA to the atmosphere is via 8:2 FTOH degradation employing a temperature-dependent rate constant of $3.2 \times 10^{-11} \times \exp^{-1000/T}$ cm^3 s^{-1} extracted from Wallington et al. [16] Similarly, "STOCH-DE" simply involved the addition of global PFOA emission data. The remainder of the simulations (STOCH-CI and STOCH-HPE) included the addition of the "Criegee Field" and the reaction of PFOA with Criegee intermediates. In short, "Criegee Field" refers to: formation reactions of SCIs from their parent alkenes, unimolecular decomposition of SCIs, bimolecular reactions of SCIs with water (and water dimer) and reaction of SCIs with PFOA. Compared with STOCHEM-CI, STOCH-HPE includes the explicit atmospheric fate of the PFOA/SCI hydroperoxide product, HPE (see Table S4 for the specific reactions and yields included in STOCH-HPE). Each simulation was run with meteorology data from 1997/98 for a period of 24 months with the first 12 months discarded as a "spin-up" year.

Table 1. Details of each simulation.

Simulation	Criegee Field Included (Y/N)	Total Species	Additional Species	No of Reactions	Additional Reactions
STOCH-Base	N	231	FTOH PFOA	532	FTOH + OH → PFOA
STOCH-DE	N	231 #	-	532	-
STOCH-CI	Y	248	SCI's *	580	SCIs formation and loss * PFOA + OH → "P1" PFOA + SCI → "P2"
STOCH-HPE	Y	249	HPE	582	PFOA + SCI→HPE ** HPE+OH→CO_2+HF HPE+OH→PFOA+HCOOH

Direct PFOA emission is included. * More details of SCI species and their formation and losses can be found in Supplementary Information (Tables S1–S3). ** The reaction product "P2" has only been replaced by "HPE."

3. Results and Discussion

3.1. Global Budget of PFOA

Table 2 provides a summary of the various simulation results. In STOCH-Base, PFOA formation from FTOH degradation is found to be 0.88 Gg $year^{-1}$. On addition of the PFOA direct emissions in the STOCH-DE, the quantification of the importance of FTOH degradation as an atmospheric source of PFOA is possible. Comparing STOCH-DE with STOCH-Base, we calculated the fraction of the

formation of PFOA via FTOH degradation, which contributes ≈15% to the total global PFOA source flux. For the STOCH-DE simulation, the modelled loss of PFOA from the atmosphere was through physical processes with wet and dry deposition contributing 80% and 20%, respectively. The contributions of both sinks decrease in the following "STOCH-CI" simulation to 71% and 19%, with the added OH and SCI-mediated oxidation processes making up the remaining 10% (8% and 2%, respectively). As the total flux through all the chemical and physical sinks, termed "Total Sink" in Table 2, remains constant in both simulations, we can assume that the oxidative loss processes occur more rapidly than the deposition processes, and thus the former simply reduce the contributions of the latter. This is also evident from the decrease in the atmospheric lifetime of PFOA seen between the "STOCH-DE" and "STOCH-CI" simulations (from 3.3 days in "STOCH-DE" to 2.9 days in "STOCH-CI"). This is in line with what we would expect given the rapid rate of reaction of PFOA with SCI and the abundances of OH radicals in the troposphere. The modelled atmospheric lifetime of PFOA following addition of the "Criegee Field" in the "STOCH-CI" simulation is considerably lower than reported literature values and that for "STOCH-DE" [23]. However, following the addition of a previously unconsidered removal process, this result is not surprising.

Table 2. Global flux data (with percentage contributions to total source/sink), global burden and lifetime of PFOA from successive simulations. The percentage contributions are shown in the parenthesis.

Simulation	STOCH-DE	STOCH-CI	STOCH-HPE
Emission (Gg year^{-1})	5.000 (≈85%)	5.000 (85%)	5.000 (≈84%)
Chemical Production (Gg year^{-1})	0.881 (≈15%)	0.881 (≈15%)	0.925 (≈16%)
Total Source (Gg year^{-1})	5.881	5.881	5.925
OH removal (Gg year^{-1})	N/A	0.442 (≈8%)	0.442 (≈8%)
Dry deposition (Gg year^{-1})	1.191 (≈20%)	1.114 (≈19%)	1.114 (≈19%)
Wet deposition (Gg year^{-1})	4.637 (≈80%)	4.170 (≈71%)	4.170 (≈71%)
Criegee removal (Gg year^{-1})	N/A	0.104 (≈2%)	0.104 (≈2%)
Total Sink (Gg year^{-1})	5.829	5.830	5.830
Global Burden (Gg)	0.053	0.046	0.047
Lifetime (days)	3.3	2.9	2.9

In the simulation, "STOCH-HPE," the chemical production of PFOA through the OH gas-phase oxidation of HPE gives a non-negligible amount of ≈0.04 Gg year^{-1} and results in a small increase in the overall global burden (≈2%). "Chemical Production" as a source of PFOA now has a slightly increased contribution of 0.925 Gg year^{-1} (≈16% compared with ≈15% in STOCH-DE simulation) to the total source of PFOA.

3.2. Surface Plots of PFOA and the Atmospheric Fate of PFOA in Terms of Its Reaction with Criegee Intermediates

The global average distribution of PFOA is presented in Figure 1a (season-specific surface distribution plots of PFOA can be found in Figure S2), where concentration peaks are shown to occur over industrial hubs (e.g., Europe, the east coast of the US and the Middle East). Figure 1b shows significant losses of PFOA as a result of reaction with SCI. This loss process is shown to be particularly significant over tropical areas where up to 90% of PFOA is shown to be removed via SCI-oxidation. Simulations utilising a Criegee field based on older kinetic information [34,53] predicted removal by SCI-mediated oxidation to be much more significant than is shown in Figure 1b, with approximately 30% of PFOA being removed as a result of this reaction over all landmass (see Figure S3 for corresponding plot). This can be explained by the rates of some atmospheric decomposition routes of SCIs (i.e., unimolecular composition and reaction with water dimer) in the new Criegee field, which is much more significant [28] than was assumed previously [53]. This result can be extended to a range of organic and halogenated acids, and as such, the atmospheric importance of these intermediates increases even further. In fact, these results suggest reaction with SCIs is likely to be a dominating

removal process of PFOA over a significant portion of landmass. Particularly in areas with high alkene concentrations (i.e., tropical regions), consideration of this loss process in models is likely to significantly alter our predictions of atmospheric concentrations of a range of compounds.

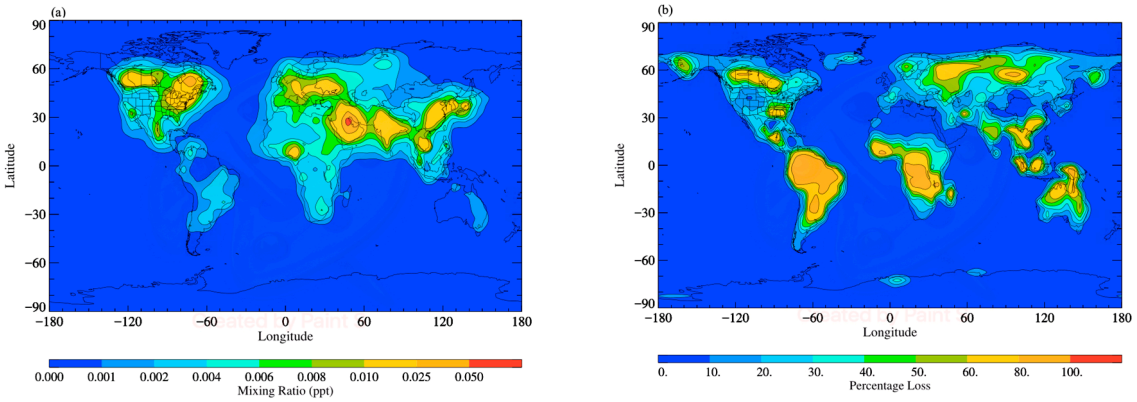

Figure 1. The surface distribution plot depicting the surface level (**a**) mixing ratios of PFOA in ppt simulated by STOCH-DE; (**b**) percentage of PFOA removed as a result of its reaction with stable Criegee intermediates (SCIs) simulated by STOCH-CI.

Despite clear concentration peaks of Criegee intermediates over the tropics, a plot of the atmospheric lifetime of PFOA with respect to SCI-mediated loss shows significant contributions over all landmasses (see Figure 2a). Of course, the shortest atmospheric lifetimes are indeed located over areas experiencing peaks in SCI concentrations (with a minimum modelled lifetime of ≈7 min over the state of Roraima in Brazil). However, in general, the lifetime upper-limit over landmasses is ≈2.5 days (in reasonable agreement with SCI-mediated lifetimes reported in the literature) [23]. Further comparison of this result with the literature indicates that a significantly shorter lifetime of PFOA is facilitated by reaction with SCIs than that facilitated by deposition (the route generally accepted as PFOA's primary loss process from the atmosphere) over all landmass.

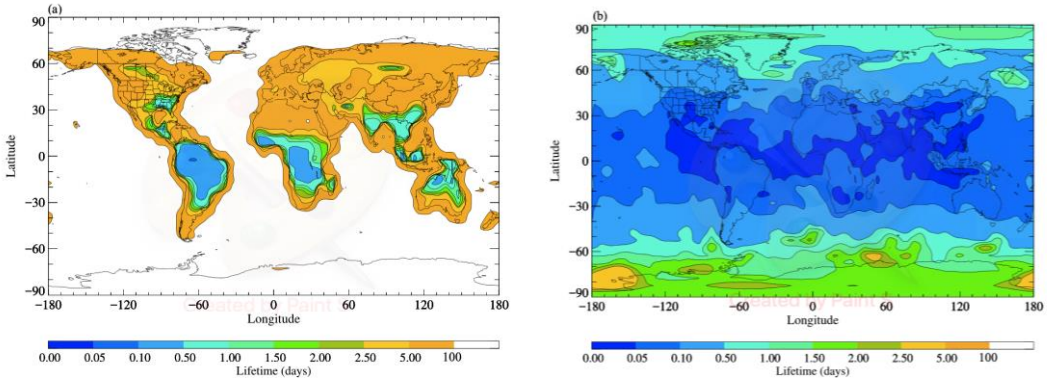

Figure 2. The surface distribution plot depicting the average lifetime of PFOA with respect to reaction with (**a**) SCIs, (**b**) SCIs and OH in days. Areas in white represent positions where the lifetime of PFOA is expected to be greater than 100 days.

Naturally, the significance of SCI-mediated removal is only apparent over landmasses; Figure 2a shows SCI-mediated removal to be negligible over bodies of water and at the South Pole. As we would expect, when considering SCI-mediated loss of PFOA exclusively, the atmospheric lifetime of PFOA increases hugely as we move away from land as SCI concentrations decrease (peaking at a maximum lifetime of over 2 years). If OH-mediated removal of PFOA alone is now considered, a much more consistent contribution to PFOA removal is observed across the globe (see Figure S4).

All loss processes are occurring simultaneously, and so a combined lifetime will be much more representative of the actual PFOA atmospheric lifetime. A surface distribution plot of the lifetime of PFOA considering both chemical loss processes is shown in Figure 2b. As is expected, the most rapid removal of PFOA is observed in the areas where SCI and OH concentration peaks intersect, and the longest lifetimes are concentrated at the poles. Combining the rate expressions for OH and SCI-mediated removal of PFOA (with rate constants of 1.7×10^{-13} cm^3 s^{-1} and 4.9×10^{-10} cm^3 s^{-1}, respectively), an overall average lifetime of ≈ 12 h is calculated (ranging from 7 min to ≈1.5 days over land). Whilst this calculated average is lower in magnitude than what has been reported previously by Taatjes et al. [23] (≈1.7 days), this is likely because their calculation only considered the reaction of PFOA with SCI chemical as the sole loss process.

Nevertheless, it is important to consider that SCI-mediated oxidation of PFOA may not necessarily represent a permanent loss of PFOA from the atmosphere. As reported by Taatjes et al., the atmospheric fate of HPE, produced from reaction of PFOA with SCIs is expected to primarily result in the regeneration of atmospheric PFOA [23]. In the first instance, this is likely to occur via hydrolysis of HPE in aqueous phases of the atmosphere (i.e., precipitation, fog, clouds). HPE is highly soluble in water (as reflected in its large Henry's law constant) [48] and also has a low vapour pressure and is thus likely to rapidly partition into atmospheric aqueous phases (on an average time-scale of 10 days) where it can undergo rapid hydrolysis to form PFOA (and SCI aqueous-phase products) [54]. The most probable effect of this is simply the acceleration of PFOA removal via wet deposition. Furthermore, any dry deposition of HPE into aqueous phases (i.e., oceans, lakes) is also likely to rapidly hydrolyse, thereby reforming PFOA. The "STOCH-HPE" simulation included deposition parameters for HPE, detailed in Table S5, and so the contributions of these routes may be considered. Whilst chemical loss of HPE from the atmosphere gave a flux of ≈ 0.061 Gg $year^{-1}$, the combined deposition flux was similarly significant at ≈ 0.054 Gg $year^{-1}$. Given the substantial contribution of deposition processes to the overall sink of HPE in the atmosphere, it becomes important to reiterate the likelihood that deposited HPE will simply result in the reformation of PFOA by biological degradation in a range of environmental aqueous phases. Unfortunately, it is very difficult to precisely account for such eventualities using the STOCHEM-CRI model, and so further investigation into this theory has not been conducted at this time.

Moving forward, as the partitioning of HPE is reversible, it is also necessary to consider its gas-phase chemistry. Inclusion of the atmospheric fate of HPE in the STOCHEM-HPE simulation results in a quantifiable increase in the chemical production of atmospheric PFOA (see Table 2). The total amount of HPE generated by PFOA undergoing SCI-mediated is ≈ 0.1 Gg $year^{-1}$. Looking at the individual loss fluxes of HPE, we see that ≈0.01 Gg of HPE goes on to be oxidised such that it results in the permanent removal of an equivalent amount of PFOA. Conversely, ≈0.04 Gg of HPE is seen to be reformed via an alternative oxidation route resulting in the reformation of PFOA. Overall, of the 0.1 Gg generated by reaction with SCIs: 0.01 Gg is oxidised such that an equivalent amount of PFOA is destroyed, 0.04 Gg reforms PFOA by oxidation and thus the fate of a further 0.05 Gg of HPE is left chemically unaccounted for. This is explained by loss of HPE via physical processes (i.e., deposition). Indeed, the combined deposition flux for HPE (≈0.054 Gg $year^{-1}$) is sufficient to explain the observed loss. Thus, as a result of SCI-mediated oxidation, a decrease of ≈ 0.06 Gg of gaseous PFOA (≈58%) is seen. However, it is important to note that whilst gaseous PFOA is reduced, deposited HPE is likely to simply result in the reformation of PFOA in the aqueous phase. This, however, cannot be properly accounted for in this gas-phase model.

The validity of this conclusion was assessed by running simulations featuring varying branching ratios of atmospheric HPE oxidation. Additional simulations were performed in which 20%, 50% or 100% of HPE was oxidised via the PFOA regeneration route (along with the original simulation assuming 80% was oxidised via this route). Despite significant changes in the branching ratios, the overall contribution of this reaction to the global burden of PFOA was much less substantial with a total variation of ≈1% across all four simulations (see Table 3). This supports the idea that whilst this

route of gaseous PFOA generation is significant, it is limited by the short atmospheric lifetime of HPE, which instead facilitates PFOA regeneration in environmental aqueous phases.

Table 3. Global burden data for PFOA across four simulations where the yield of the PFOA-reforming oxidation of HPE was varied between 20% and 100%.

Yield of PFOA Reformation Reaction	PFOA Global Burden (Gg)
20%	0.0464
50%	0.0466
80%	0.0468
100%	0.0469

3.3. Measurement Data Comparison

Comparing model output to measurement data is unquestionably an essential part of evaluating a model's accuracy. However, despite being a compound of significant scientific interest, comprehensive measurement data of PFOA atmospheric concentrations are scarce in the literature. This is even more the case for SCI atmospheric concentrations, though in this instance it is as a result of the extremely low steady-state concentrations of these species. This lack of measurement data makes complete evaluation of the model challenging nevertheless comparison with available data provides promising agreement.

For PFOA, one of the few complete data sets for gas-phase atmospheric PFOA concentrations in the literature have been reported by Harada et al. [55]. Whilst comparison of model output with these data (see Figure 3a) is still valid, the area where the data collection took place (Oyamazaki, Kyoto) was noted to have a significant source of PFOA pollution compared with other areas of Kyoto. As a result of the limitations from the coarse resolution (5° × 5°) of the model, it is likely that most simulations will under predict PFOA concentrations significantly. As such, the measured data from Harada et al. have been reduced to 50% of their original value to allow for comparison to model output.

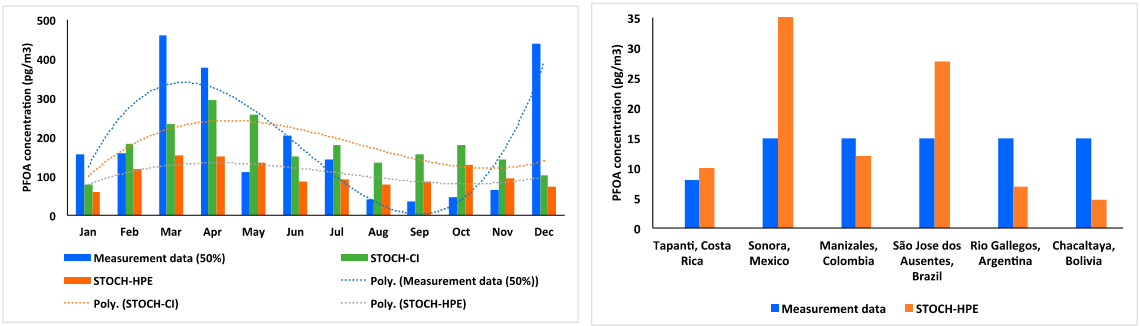

(**a**) (**b**)

Figure 3. (**a**) A histogram showing a comparison between the measurement data collected by Harada et. al. [55] (reduced to 50% to account for the pollution of the measured environment) and model outputs for the "STOCH-CI" and "STOCH-HPE" simulations. Third -order polynomial trend lines have been imposed on each dataset to allow for an arbitrary comparison of seasonality. (**b**) A histogram showing a comparison between the measurement data collected from Rauert et al. [56] and model outputs for the "STOCH-HPE" simulation. For all sites, excluding Costa Rica, PFOA was not detected above the method detection limit (15 pg m^{-3}).

Whilst this anticipated under-prediction was seen in all simulations, data seasonality was replicated within a reasonable degree of accuracy in simulations including the Criegee field. Small discrepancies in seasonality replication may be attributed to the use of dated climatological data, given the importance of deposition as a route of removal of PFOA from the atmosphere. Interestingly, despite an overall

increase in the global burden of PFOA between the STOCH-CI and the STOCH-HPE simulations, in this area we see a decrease in modelled PFOA. This is likely due to efficient deposition of HPE—indeed, this area sees significant rainfall throughout the year—which would reduce the gaseous concentration of PFOA (though will not result in the permanent removal of PFOA from the environment).

A further measurement study, reported by Rauert et al. [56], collected PFOA concentration data from a range of locations in the GRULAC region (Group of Latin America and Caribbean). Here we see good model-measurement agreement between the sites in Costa Rica, Colombia, Argentina and Bolivia (see Figure 3b). For other sites, in Mexico and Brazil, we see an overestimation in the model. This is likely to be due to underestimations of the Criegee concentrations in these areas. Indeed, comparison between this study and one using a dated Criegee field approximation shows large discrepancies between the predicted concentrations over tropical forested regions. It is likely that the true magnitude of the Criegee Field lies somewhere between that predicted by these two studies; as we get closer to the true value, model-measurement agreement is likely to continue to improve.

4. Conclusions

The aim of this investigation was to ascertain the impact of an updated chemical mechanism within STOCHEM-CRI on the simulated atmospheric production, fate and transport of PFOA. A range of simulations were performed, and the results were analysed as thoroughly as possible using the limited measurement and modelling data available in the literature. The inclusion of the "Criegee Field" is a significant addition to the previous chemical mechanism and has proven to be a significant loss process for PFOA in the atmosphere. The reaction with SCIs is responsible for up to 90% of the chemical loss of PFOA. However, the results of this investigation indicate that reaction of PFOA with SCIs in the atmosphere may not be a significant long-term sink, given that ≈42% of the generated product subsequently degrades in the atmosphere, reforming the PFOA. Nevertheless, further investigation into sink-specific contributions suggests that the HPE product from reaction of PFOA with SCIs is removed via deposition processes at a similar flux to that by atmospheric degradation. It can therefore be stated that the simulated atmospheric concentration of PFOA does indeed decrease as a result of the addition of the "Criegee Field" (though, in reality, it is likely that HPE simply degrades to PFOA in environmental aqueous phases as opposed to in the gas-phase).

Due to the resolution limits of global modelling techniques, underestimation of PFOA concentrations in polluted environments persist throughout the simulation results. Despite this, successive simulations continued to show improvement with regard to seasonal variation in available measurement data. Correspondingly, any further modelling investigations into the atmospheric fate of PFOA would become considerably more meaningful with a corresponding increase in gas-phase measurement data.

Supplementary Materials: The following are available online at http://www.mdpi.com/2073-4433/11/4/407/s1. Table S1: Stabilised Criegee intermediates added as part of the inclusion of the "Criegee Field" in the STOCHEM chemical module [28], Table S2: Complete set of the 26 SCI formation reactions included in the STOCHEM chemical module [53], Table S3: Complete set of the 24 SCI loss reactions included in the STOCHEM chemical module [28], Table S4: The reactions depicting the potential chemical degradation routes of HPE in the atmosphere [23], Table S5: The deposition parameters included for HPE in the STOCHEM-HPE [57], Figure S1: The schematic diagram of the formation and loss reactions of PFOA, Figure S2: The surface distribution plot depicting the surface level percentage of PFOA removed as a result of its reaction with SCIs [34,53], Figure S3: The surface distribution plot depicting the surface level mixing ratios of PFOA in parts per trillion (ppt) for (a) the northern hemispheric summer months (June-July-August) and (b) the northern hemispheric winter months (December-January-February), Figure S4: The surface distribution plot depicting the average lifetime of PFOA with respect to reaction with OH in days.

Author Contributions: R.H. performed the model runs, analysed the modelled data and wrote the paper; M.A.H.K. and D.E.S. designed the project and wrote the paper; R.C.-P., A.J.O.-E., C.J.P. and C.A.T. provided experimental kinetic data and gave feedback to improve the manuscript. All authors have read and agreed to the published version of the manuscript.

Funding: Natural Environment Research Council (NERC) (grants NE/K004905/1, NE/I014381/1 and NE/P013104/1), Primary Science Teaching Trust.

Acknowledgments: We thank the NERC (grants NE/K004905/1, NE/I014381/1 and NE/P013104/1) and the Bristol ChemLabS and Primary Science Teaching Trust under whose auspices various aspects of this work were funded. C.J.P.'s work was carried out at Jet Propulsion Laboratory, California Institute of Technology, under contract with the National Aeronautics and Space Administration (NASA), and was supported by the Upper Atmosphere Research and Tropospheric Chemistry Programs. The participation of C.A.T. is supported by the Office of Chemical Sciences, Geosciences, and Biosciences, Office of Basic Energy Sciences, United States Department of Energy. Sandia National Laboratories is a multi-mission laboratory managed and operated by National Technology and Engineering Solutions of Sandia, LLC., a wholly owned subsidiary of Honeywell International, Inc., for the U.S. Department of Energy's National Nuclear Security Administration under contract DE-NA0003525 (The Advanced Light Source is supported by the Director, Office of Science, Office of Basic Energy Sciences, of the U.S. Department of Energy under Contract No. DE-AC02-05CH11231). The views expressed in the article do not necessarily represent the views of the U.S. Department of Energy or the United States Government.

Conflicts of Interest: The authors declare no conflict of interest.

References

1. Ellis, D.A.; Moody, C.A.; Mabury, S.A. Organofluorines. In *The Handbook of Environmental Chemistry*; Nielson, A., Ed.; Springer: Heidelberg, Germany, 2002; Chapter 3, Part N.
2. Yamashita, N.; Kannan, K.; Taniyasu, S.; Horii, Y.; Petrick, G.; Gamo, T. A global survey of perfluorinated acids in oceans. *Mar. Pollut. Bull.* **2005**, *51*, 658–668. [CrossRef] [PubMed]
3. Martin, J.W.; Smithwick, M.M.; Braune, B.M.; Hoekstra, P.F.; Muir, D.C.G.; Mabury, S.A. Identification of long-chain perfluorinated acids in biota from the Canadian Arctic. *Environ. Sci. Technol.* **2004**, *38*, 373–380. [CrossRef] [PubMed]
4. Berthiaume, J.; Wallace, K.B. Perfluorooctanoate, perfluorooctanesulfonate, and N-ethylperfluorooctanesulfonamido ethanol; peroxisome proliferation and mitochondrial biogenesis. *Toxicol. Lett.* **2002**, *129*, 23–32. [CrossRef]
5. Upham, B.L.; Deocampo, N.D.; Wurl, B.; Trosko, J.E. Inhibition of gap junctional intercellular communication by perfluorinated fatty acids is dependent on the chain length of the fluorinated tail. *Int. J. Cancer* **1998**, *78*, 491–495. [CrossRef]
6. Wang, Z.; Cousins, I.T.; Scheringer, M.; Buck, R.C.; Hungerbühler, K. Global emission inventories for C_4–C_{14} perfluoroalkyl carboxylic acid (PFCA) homologues from 1951 to 2030, part II: The remaining pieces of the puzzle. *Environ. Int.* **2014**, *69*, 166–176. [CrossRef]
7. EWG. PFCs: Global Contaminants. Available online: https://www.ewg.org/research/pfcs-global-contaminants (accessed on 18 March 2020).
8. Kannan, K.; Corsolini, S.; Falandysz, J.; Fillmann, G.; Kumar, K.S.; Loganathan, B.G.; Mohd, M.A.; Olivero, J.; Wouwe, N.V.; Yang, J.H.; et al. Perfluorooctanesulfonate and related fluorochemicals in human blood from several countries. *Environ. Sci. Technol.* **2004**, *38*, 4489–4495. [CrossRef]
9. Sturm, R.; Ahrens, L. Trends of polyfluoroalkyl compounds in marine biota and in humans. *Environ. Chem.* **2010**, *7*, 457–484. [CrossRef]
10. Dietz, R.; Bossi, R.; Rigét, F.F.; Sonne, C.; Born, E.W. Increasing perfluoroalkyl contaminants in East Greenland polar bears (*Ursus maritimus*): A new toxic threat to the Arctic bears. *Environ. Sci. Technol.* **2008**, *42*, 2701–2707. [CrossRef]
11. EPA. Health Effects Support Document for Perfluorooctanoic Acid (PFOA). EPA 822-R-16-003; 2016. Available online: www.epa.gov/ground-water-and-drinking-water/supporting-documents-drinking-water-health-advisories-pfoa-and-pfos (accessed on 18 March 2020).
12. Stemmler, I.; Lammel, G. Pathways of PFOA to the Arctic: Variabilities and contributions of oceanic currents and atmospheric transport and chemistry sources. *Atmos. Chem. Phys.* **2010**, *10*, 9965–9980. [CrossRef]
13. Xie, Z.; Wang, Z.; Mi, W.; Möller, A.; Wolschke, H.; Ebinghaus, R. Neutral poly-/perfluoroalkyl substances in air and snow from the Arctic. *Sci. Rep.* **2015**, *5*, 8912. [CrossRef]
14. EPA. Technical Fact Sheet- Perfluorooctane Sulfonate (PFOS) and Perfluorooctanoic Acid (PFOA). EPA 505-F-17-001; United States Environmental Protection Agency, 2017. Available online: https://www.epa.gov/sites/production/files/2017-12/documents/ffrrofactsheet_contaminants_pfos_pfoa_11-20-17_508_0.pdf (accessed on 18 March 2020).
15. Programme, U.E. The New POPs under the Stockholm Convention. Available online: http://chm.pops.int/TheConvention/ThePOPs/TheNewPOPs/tabid/2511/Default.aspx (accessed on 20 March 2020).

16. Wallington, T.J.; Hurley, M.D.; Xia, J.; Wuebbles, D.J.; Sillman, S.; Ito, A.; Penner, J.E.; Ellis, D.A.; Martin, J.; Mabury, S.A.; et al. Formation of C7F15COOH (PFOA) and other perfluorocarboxylic acids during the atmospheric oxidation of 8:2 fluorotelomer alcohol. *Environ. Sci. Technol.* **2006**, *40*, 924–930. [CrossRef] [PubMed]
17. Ellis, D.A.; Martin, J.W.; De Silva, A.O.; Mabury, S.A.; Hurley, M.D.; Andersen, M.P.S.; Wallington, T.J. Degradation of fluorotelomer alcohols: A likely atmospheric source of perfluorinated carboxylic acids. *Environ. Sci. Technol.* **2004**, *38*, 3316–3321. [CrossRef] [PubMed]
18. Zhao, Z.; Tang, J.; Mi, L.; Tian, C.; Zhong, G.; Zhang, G.; Wang, S.; Li, Q.; Ebinghaus, R.; Xie, Z.; et al. Perfluoroalkyl and polyfluoroalkyl substances in the lower atmosphere and surface waters of the Chinese Bohai Sea, Yellow Sea, and Yangtze River estuary. *Sci. Total Environ.* **2017**, *599*, 114–123. [CrossRef] [PubMed]
19. Dorman, F.L.; Reiner, E.J. Chapter 28—Emerging and persistent environmental compound analysis. In *Gas Chromatography*; Poole, C.F., Ed.; Elsevier: Amsterdam, The Netherlands, 2012; pp. 647–677.
20. Ellis, D.A.; Martin, J.W.; Mabury, S.A.; Hurley, M.D.; Andersen, M.P.S.; Wallington, T.J. Atmospheric lifetime of fluorotelomer alcohols. *Environ. Sci. Technol.* **2003**, *37*, 3816–3820. [CrossRef]
21. Vierke, L.; Staude, C.; Biegel-Engler, A.; Drost, W.; Schulte, C. Perfluorooctanoic acid (PFOA)—Main concerns and regulatory developments in Europe from an environmental point of view. *Environ. Sci. Eur.* **2012**, *24*, 16. [CrossRef]
22. Wang, Y.; Zhang, P. Effects of pH on photochemical decomposition of perfluorooctanoic acid in different atmospheres by 185 nm vacuum ultraviolet. *J. Environ. Sci.* **2014**, *26*, 2207–2214. [CrossRef]
23. Taatjes, C.A.; Khan, M.A.H.; Eskola, A.J.; Percival, C.J.; Osborn, D.L.; Wallington, T.J.; Shallcross, D.E. Reaction of perfluorooctanoic acid with Criegee intermediates and implications for the atmospheric fate of perfluorocarboxylic acids. *Environ. Sci. Technol.* **2019**, *53*, 1245–1251. [CrossRef]
24. Houde, M.; Martin, J.W.; Letcher, R.J.; Solomon, K.R.; Muir, D.C.G. Biological monitoring of polyfluoroalkyl substances: A review. *Environ. Sci. Technol.* **2006**, *40*, 3463–3473. [CrossRef]
25. Armitage, J.M.; MacLeod, M.; Cousins, I.T. Comparative assessment of the global fate and transport pathways of long-chain perfluorocarboxylic acids (PFCAs) and perfluorocarboxylates (PFCs) emitted from direct sources. *Environ. Sci. Technol.* **2009**, *43*, 1134–1140. [CrossRef]
26. Vereecken, L.; Novelli, A.; Taraborrelli, D. Unimolecular decay strongly limits the atmospheric impact of Criegee intermediates. *Phys. Chem. Chem. Phys.* **2017**, *19*, 31599–31612. [CrossRef]
27. Khan, M.A.H.; Percival, C.J.; Caravan, R.L.; Taatjes, C.A.; Shallcross, D.E. Criegee intermediates and their impacts on the troposphere. *Environ. Sci. Process. Impacts* **2018**, *20*, 437–453. [CrossRef] [PubMed]
28. Chhantyal-Pun, R.; Khan, M.A.H.; Martin, R.; Zachhuber, N.; Buras, Z.J.; Percival, C.J.; Shallcross, D.E.; Orr-Ewing, A.J. Direct kinetic and atmospheric modeling studies of Criegee intermediate reactions with acetone. *ACS Earth Space Chem.* **2019**, *3*, 2363–2371. [CrossRef]
29. Lin, J.M., Jr.; Chao, W. Structure-dependent reactivity of Criegee intermediates studies with spectroscopic methods. *Chem. Soc. Rev.* **2017**, *46*, 7483–7497. [CrossRef]
30. Taatjes, C.A. Criegee intermediates: What direct production and detection can teach us about reactions of carbonyl oxides. *Annu. Rev. Phys. Chem.* **2017**, *68*, 183–207. [CrossRef]
31. Welz, O.; Eskola, A.J.; Sheps, L.; Rotavera, B.; Savee, J.D.; Scheer, A.M.; Osborn, D.L.; Lowe, D.; Booth, A.M.; Xiao, P.; et al. Rate coefficients of Criegee intermediate (CH_2OO and CH_3CHOO) reactions with formic and acetic acid are close to their collision limit: Direct kinetics measurements and atmospheric implications. *Angew. Chem. Int. Ed.* **2014**, *53*, 4547–4550. [CrossRef] [PubMed]
32. Foreman, E.S.; Kapnas, K.M.; Murray, C. Reactions between Criegee intermediates and the inorganic acids HCl and HNO_3: Kinetics and atmospheric implications. *Angew. Chem. Int. Ed.* **2016**, *55*, 10419–10422. [CrossRef]
33. Chhantyal-Pun, R.; McGillen, M.R.; Beames, J.M.; Khan, M.A.H.; Percival, C.J.; Shallcross, D.E.; Orr-Ewing, A.J. Temperature dependence of the rates of reaction of trifluoroacetic acid with Criegee intermediates. *Angew. Chem. Int. Ed.* **2017**, *56*, 9044–9047. [CrossRef]
34. Chhantyal-Pun, R.; Rotavera, B.; McGillen, M.R.; Khan, M.A.H.; Eskola, A.J.; Caravan, R.L.; Blacker, L.; Tew, D.P.; Osborn, D.L.; Percival, C.J.; et al. Criegee intermediate reactions with carboxylic acids: A potential source of secondary organic aerosol in the atmosphere. *ACS Earth Space Chem.* **2015**, *2*, 833–842. [CrossRef]
35. Østerstrøm, F.; Wallington, T.J.; Andersen, M.; Nielsen, O.J. Atmospheric chemistry of $(CF_3)_2CHOCH_3$, $(CF_3)_2CHOCHO$, and $CF_3C(O)OCH_3$. *J. Phys. Chem. A* **2015**, *119*, 10540–10552. [CrossRef]

36. Collins, W.J.; Stevenson, D.S.; Johnson, C.E.; Derwent, R.G. Tropospheric ozone in a global-scale three-dimensional Lagrangian model and its response to NOx emission controls. *J. Atmos. Chem.* **1997**, *26*, 223–274. [CrossRef]
37. Johns, T.C.; Carnell, R.E.; Crossley, J.F.; Gregory, J.M.; Mitchell, J.F.B.; Senior, C.A.; Tett, S.F.B.; Wood, R.A. The second Hadley Centre coupled ocean-atmosphere GCM: Model description, spinup and validation. *Clim. Dyn.* **1997**, *13*, 103–134. [CrossRef]
38. Khan, M.A.H.; Cooke, M.C.; Utembe, S.R.; Archibald, A.T.; Maxwell, P.; Morris, W.C.; Xiao, P.; Derwent, R.G.; Jenkin, M.E.; Percival, C.J.; et al. A study of global atmospheric budget and distribution of acetone using global atmospheric model STOCHEM-CRI. *Atmos. Environ.* **2015**, *112*, 269–277.
39. Derwent, R.G.; Stevenson, D.S.; Doherty, R.M.; Collins, W.J.; Sanderson, M.G. How is surface ozone in Europe linked to Asian and North American NO_x emissions? *Atmos. Environ.* **2008**, *42*, 7412–7422.
40. Jenkin, M.E.; Watson, L.A.; Utembe, S.R.; Shallcross, D.E. A Common Representative Intermediate (CRI) mechanism for VOC degradation. Part-1: Gas phase mechanism development. *Atmos. Environ.* **2008**, *42*, 7185–7195.
41. Watson, L.A.; Shallcross, D.E.; Utembe, S.R.; Jenkin, M.E. A Common Representative Intermediate (CRI) mechanism for VOC degradation. Part 2: Gas phase mechanism reduction. *Atmos. Environ.* **2008**, *42*, 7196–7204.
42. Utembe, S.R.; Watson, L.A.; Shallcross, D.E.; Jenkin, M.E. A Common Representative Intermediates (CRI) mechanism for VOC degradation. *Atmos. Environ.* **2009**, *43*, 1982–1990.
43. Utembe, S.R.; Cooke, M.C.; Archibald, A.T.; Jenkin, M.E.; Derwent, R.G.; Shallcross, D.E. Using a reduced Common Representative Intermediates (CRI v2-R5) mechanism to simulate tropospheric ozone in a 3-D Lagrangian chemistry transport model. *Atmos. Environ.* **2010**, *44*, 1609–1622.
44. Khan, M.A.H.; Jenkin, M.E.; Foulds, A.; Derwent, R.G.; Percival, C.J.; Shallcross, D.E. A modeling study of secondary organic aerosol formation from sesquiterpenes using the STOCHEM global chemistry and transport model. *J. Geophys. Res. Atmos.* **2017**, *122*, 4426–4439.
45. Khan, A.; Razis, B.; Gillespie, S.; Percival, C.; Shallcross, D. Global analysis of carbon disulfide (CS_2) using the 3-D chemistry transport model STOCHEM. *Aims Environ. Sci.* **2017**, *4*, 484–501.
46. Percival, C.J.; Welz, O.; Eskola, A.J.; Savee, J.D.; Osborn, D.L.; Topping, D.O.; Lowe, D.; Utembe, S.R.; Bacak, A.; McFiggans, G.; et al. Regional and global impacts of Criegee intermediates on atmospheric sulfuric acid concentrations and first steps of aerosol formation. *Faraday Discuss.* **2013**, *165*, 45–73.
47. Von Kuhlmann, R.; Lawrence, M.G.; Crutzen, P.J.; Rasch, P.J. A model for studies of tropospheric ozone and nonmethane hydrocarbons: Model description and ozone results. *J. Geophys. Res. Atmos.* **2003**, *108*, 4294.
48. Sander, R. Compilation of Henry's law constants (version 4.0) for water as solvent. *Atmos. Chem. Phys.* **2015**, *15*, 4399–4981.
49. Penner, J.E.; Atherton, C.S.; Graedel, T.E. Global Emissions and Models of Photochemically Active compounds. In *Global Atmospheric-Biospheric Chemistry*; Prinn, R.G., Ed.; Springer: Berlin/Heidelberg, Germany, 1994; Volume 48, pp. 223–247.
50. Dinglasan, M.J.A.; Ye, Y.; Edwards, E.A.; Mabury, S.A. Fluorotelomer alcohol biodegradation yields poly- and perfluorinated acids. *Environ. Sci. Technol.* **2004**, *38*, 2857–2864. [CrossRef] [PubMed]
51. Khan, M.A.H.; Cooke, M.C.; Utembe, S.R.; Xiao, P.; Derwent, R.G.; Jenkin, M.E.; Archibald, A.T.; Maxwell, P.; Morris, W.C.; South, N.; et al. Reassessing the photochemical production of methanol from peroxy radical self and cross reactions using the STOCHEM-CRI global chemistry and transport model. *Atmos. Environ.* **2014**, *99*, 77–84. [CrossRef]
52. Master Chemical Mechanism (MCM), ver. 3.2. Available online: http://mcm.leeds.ac.uk/MCM (accessed on 18 March 2020).
53. McGillen, M.R.; Curchod, B.F.E.; Chhantyal-Pun, R.; Beames, J.M.; Watson, N.; Khan, M.A.H.; McMahon, L.; Shallcross, D.E.; Orr-Ewing, A.J. Criegee intermediate-alcohol reactions, a potential source of functionalized hydroperoxides in the atmosphere. *ACS Earth Space Chem.* **2017**, *1*, 664–672. [CrossRef]
54. Zhao, R.; Kenseth, C.M.; Huang, Y.; Dalleska, N.F.; Kuang, X.M.; Chen, J.; Paulson, S.E.; Seinfeld, J.H. Rapid aqueous-phase hydrolysis of ester hydroperoxides arising from Criegee intermediates and organic acids. *J. Phys. Chem. A* **2018**, *122*, 5190–5201. [CrossRef] [PubMed]
55. Harada, K.; Nakanishi, S.; Saito, N.; Tsutsui, T.; Koizumi, A. Airborne perfluorooctanoate may be a substantial source contamination in Kyoto area, Japan. *Bul. Environ. Contam. Toxicol.* **2005**, *74*, 64–69. [CrossRef]

56. Rauert, C.; Harner, T.; Schuster, J.K.; Eng, A.; Fillmann, G.; Castillo, L.E.; Fentanes, O.; Ibarra, M.V.; Miglioranza, K.S.B.; Rivadeneira, I.M.; et al. Atmospheric concentrations of New Persistent Organic Pollutants and Emerging Chemicals of Concern in the Group of Latin America and Caribbean (GRULAC) region. *Environ. Sci. Technol.* **2018**, *52*, 7240–7269. [CrossRef]
57. Hough, A.M. Development of a two-dimensional global tropospheric model: Model chemistry. *J. Geophys. Res. Atmos.* **1991**, *96*, 7325–7362.